

# CCD testing and characterization for Dark Energy Survey

J. Estrada<sup>1</sup>, T. Abbott<sup>2</sup>, B. Ansgardt<sup>1</sup>, L. Buckley-Geer<sup>1</sup>, M. Brown<sup>3</sup>, J. Campa<sup>4</sup>, L. Cardiel<sup>4</sup>, H. Cease<sup>1</sup>, B. Flaugher<sup>1</sup>, K. Dawson<sup>5</sup>, G. Derylo<sup>1</sup>, H.T. Diehl<sup>1</sup>, S. Gruenendahl<sup>1</sup>, I. Karliner<sup>6</sup>, W. Merrit<sup>1</sup>, P. Moore<sup>2</sup>, T.C. Moore<sup>6</sup>, N. Roe<sup>5</sup>, V. Scarpine<sup>1</sup>, R. Schmidt<sup>2</sup>, M. Schubnel<sup>3</sup>, T. Shaw<sup>1</sup>, W. Stuermer<sup>1</sup> and J. Thaler<sup>6</sup>.

<sup>1</sup>Fermi National Accelerator Laboratory<sup>a</sup>, Batavia, IL, USA

<sup>2</sup>Cerro Tololo Inter-American Observatory, La Serena, Chile

<sup>3</sup>University of Michigan, Ann Arbor, MI, USA

<sup>4</sup>Institut d'Estudis Espacials de Catalunya, Barcelona, Spain

<sup>5</sup>Lawrence Berkeley National Laboratory, CA, USA

<sup>6</sup>Univertisy of Illinois at Urbana-Champaign, Urbana, IL, USA

A description of the plans and infrastructure developed for CCD testing and characterization for the DES focal plane detectors is presented. Examples of the results obtained are shown and discussed in the context of the device requirements for the survey instrument.

keywords: Mosaic, CCD, DES

## 1. INTRODUCTION

The DES collaboration [1] was established with the objective of developing a new instrument for the Blanco 4 meter telescope at Cerro Tololo Inter-American Observatory (CTIO) [2] in partnership with NOAO. The project consists of building a 520 megapixel CCD camera (DECam) and wide field optical corrector for the prime focus. The DES collaboration will use this instrument as a survey instrument during 525 nights at Blanco between Oct. and Feb. during the years 2010 and 2015, the new camera will be available the remaining 70% of the time to other users for their own programs. The main science goal for DES is the measurement of  $w$ , the dark energy equation of state, to a statistical precision of order  $\delta w \leq 5\%$ .

Our survey goals require that we have high quantum efficiency (QE) at the near infrared wavelength of  $\sim 1000$  nm. The standard astronomical CCDs typically have a QE at this wavelength of 5-10% because the charge collection region is 10-20  $\mu\text{m}$  thick and the total device thickness is often less than 50  $\mu\text{m}$ . The absorption length in silicon is 205  $\mu\text{m}$  at a wavelength of 1000 nm and thus thick sensors are required for a better QE at that wavelength. LBNL has developed thick, fully depleted, back illuminated CCDs 200-300  $\mu\text{m}$  thick [4]. For DES, we will use 250  $\mu\text{m}$  thick LBNL CCDs. The DES focal plane will include 62 CCDs to cover a total active area of 3.0  $\text{deg}^2$ . Each device with 2k x 4k format has 15  $\mu\text{m}$  square pixels and is fitted with two readout amplifiers.

Every device to be installed in the DES focal plane will be first characterized in the CCD testing facility at Fermi National Accelerator Laboratory (Fermilab). Testing and grading activities include an initial phase where CCDs are exercised and characterized and a production phase where the production devices will be characterized to determine the best ones that should populate the focal plane. The initial phase is important to develop the infrastructure and experience so that the production phase may begin when production devices first become available. The production phase will be designed to test up to 20 devices per month, with some capacity to absorb bursts of higher delivery rates.

The DES CCDs will arrive at Fermilab diced and ready for packaging in the Fermilab Silicon Detector Facility (SiDet). A production lot is composed of 24 wafers. A description of the production process is included in Ref [3], the initial steps are done at Dalsa and the devices then go to LBNL for the final

---

<sup>a</sup> Operated by Universities Research Association Inc. under Contract No. DE-AC02-76CH03000 with the United States Department of Energy.

processing steps. From each lot the Dalsa requires to have 3 control wafers fully processed at their installations. These special devices are 650  $\mu\text{m}$  thick instead of the DES standard (250  $\mu\text{m}$ ). In general they will arrive at Fermilab before the fully processed ones from the same lot (approximately one month earlier) and will be tested as an early probe to the performance of the devices in a new lot. Packaging of the devices will also be done at Fermilab Silicon Detector facility, details of this process are presented in Ref [5].

In addition to four 2k x 4k devices that will populate the focal plane, each DES wafer also has smaller devices: 2k x 2k (1 per wafer) and 0.5k x 1k (8 per wafer). Details of the DES wafers are presented in Ref [3]. We do not plan to fully characterize all of the non-standard size devices, instead we will use them for packaging tests and to do special studies for which we need devices that satisfy all the science requirements but do not need to be full size, this will allow to perform these studies without compromising any device that could potentially be installed in our focal plane. A fraction of the small devices will be used for guiding and focusing in our instrument.

The DES CCD technical specifications, established as the minimal requirements in order to achieve the science goals for the survey, are discussed in some detail in Ref [6]. A slightly updated version of the requirements is presented in Table 1. The characterization for each device is consists basically in making a comparison of the performance for each CCD against the device requirements.

**Table 1. CCD requirements for DES**

	LBNL CCD performance	DES requirements
Pixel array	2048 $\times$ 4096 pixels	2048 $\times$ 4096 pixels
Pixel size	15 $\mu\text{m}$ $\times$ 15 $\mu\text{m}$	15 $\mu\text{m}$ $\times$ 15 $\mu\text{m}$ (nominal)
<QE (400-700 nm)>	~70%	>60%
<QE (700-900 nm)>	~90%	>80%
<QE (900-1000 nm)>	~60%	>50% at 1000 nm
Full well capacity	170,000 $e^-$	>130,000 $e^-$
Dark current	2 $e^-$ /hr/pixel at $-150^\circ\text{C}$	<~25 $e^-$ /hr/pixel
Persistence	Erase mechanism	Erase mechanism
Read noise	7 $e^-$ @ 250 kpix/s	< 10 $e^-$ @ 250 kpix/sec
Charge Transfer Inefficiency	< $10^{-6}$	< $10^{-5}$
Charge diffusion	6 $\mu\text{m}$	< 7 $\mu\text{m}$ (*)
Linearity	Better than 1%	1%

(\*) After a reconsideration of the PSF budget for the survey, this requirement was moved from 10  $\mu\text{m}$  in Ref. [6] to its current value.

In what follows the CCD testing activities at Fermilab are described in detail. It should be noted that even though we expect the core of the device characterization being done at Fermilab, DES also plans to have other testing stations outside Fermilab. The DES Spanish Consortium, University of Michigan and Cerro Tololo International Observatory are building testing stations to contribute to this effort.

## 2. CCD TESTING FACILITY

In order to accomplish the CCD testing goals we have built a device testing facility at Fermilab. Our original estimations of yield is 25% which means that we will need to test and fully characterize approximately 240 devices to obtain 70 scientific grade CCDs for installation in the DECam focal plane (including spares). We plan for a testing rate of approximately 5 CCDs per week. For this purpose a special area of the Silicon Detector (SiDet) facility at Fermilab has been adapted for CCD operation. This includes controlled high (>40%) humidity, extensive ESD safety equipment and automated LN2 supply (this last item still under construction).

The plan for DES CCD testing activities includes building a full scale camera vessel dedicated to study the system problems involved with the operation of a large focal plane. The operation of this full scale testing prototype is planned to start in summer 2006 and more details can be found in Ref. [3]. This document does not cover the aspects of testing involved in the full scale camera prototype.

## 2.1 CCD testing dewars

Our CCD testing laboratory at Fermilab includes three dewars like the one shown in Fig. 1. The dewars are cooled with LN2 and can be controlled to maintain a stable temperature (with less than 0.1K peak-to-peak fluctuations) using independent PID loops. We have successfully operated these dewars in temperatures that range between -50C and -160C. This large range of stable operating points is possible with a similar heating power because the design of the dewar has a valve to control the flow of boiling Nitrogen gas, effectively setting the level of LN2 inside the dewar and in this way regulating the cooling power provided by the liquid.

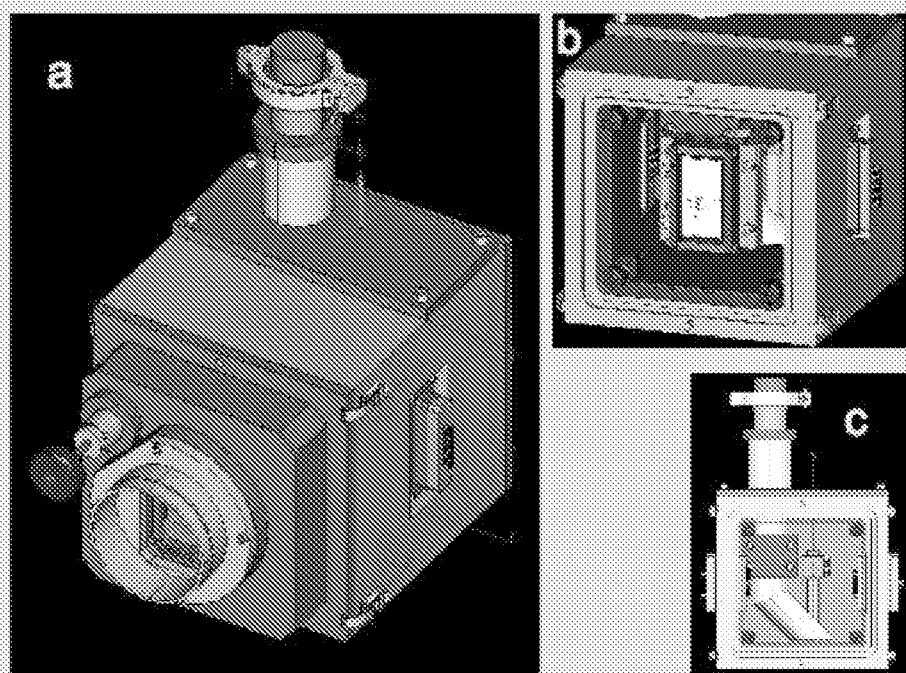


Fig.1 Drawings for the CCD testing dewar. a) Dewar fully assembled, LN2 is introduced from the top and the large window allows for a complete illumination of the 6cm x 3cm CCD (4 kpix x 2 kpix). b) Front cover is removed, the drawing shows a CCD inside mounted in the DES pedestal package (that we plan to use for the instrument [5] ). The exterior walls of the dewar are made out of Al, in the inside there is a Cu box isolates the cold parts from the exterior walls. c) View from front without cold plate and cold finger to mount the CCD, the small diameter tube is used to vent the evaporated nitrogen, a valve is used to control the flow of gas, setting in this way the level of LN2 inside the dewar.

The design of the dewar shown in Fig. 1 allows for a quick exchange of CCDs, which is a very important ingredient for the rate of testing that we need to achieve for this project. The dewar has manual clamps that can be loosened by hand (without any tools) and give clear access to the front, where the CCD is installed. Typically, once a CCD is loaded in the dewar it takes about 1 hour to produce a vacuum better than  $10^{-5}$  Torr, at that point LN2 can be loaded and approximately 2 hours later we achieve the stable operating conditions at -130 C. The forced warm up (warm up when the dewar is full on LN2) is done with a 20 watt heater that is installed in the Cu-Box as shown in Fig. 1 (see Fig. 1.b).

## 2.2. Optical equipment

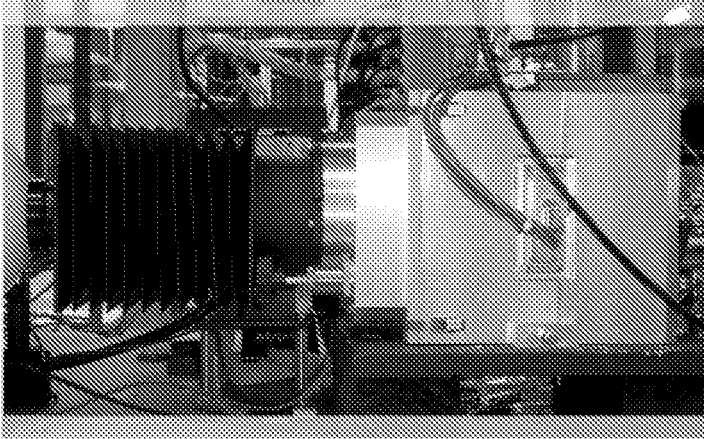


Fig. 2. Photograph of testing dewar in our CCD testing lab. The dewar is connected to a 6 inch integrating sphere using bellows, the large distance (13') between the sphere's port and the CCD allows us to produce a flat field in the entire surface of the device.

The optical equipment in our testing stations is based on the Newport/ORIEL catalog. Each dewar is illuminated by a 6'' general purpose integrating sphere with three ports. The illumination source is connected on the input port, a photodiode is connected on one of the output ports and the other output port is connected to the dewar. The CCDs that we are going to use for the DES focal plane are rectangular with dimensions 3cm x 6cm, the 6'' sphere has a 1.5'' output port, which means that we need to keep a significant distance between the CCD and the port in order to achieve flat illumination over the whole area of our detector. For this purpose we built a baffle to connect the dewar to the integrating sphere keeping 13'' distance between the sphere's port and the CCD. The dewar connected to the integrating sphere using our baffle is shown in Fig. 2. Our studies indicate that the deviations from a flat field are less than 5% on the edges of the CCD.

For the illumination source we use a broad band illumination lamp (halogen) that we can either mount directly at the input of the integrating sphere (though a mechanical shutter) or connect to a filter wheel or monochromator (also from ORIEL) to select wavelength.

Every part of our optical instrumentation is controllable by GPIB. This gives us the ability to fully automate the CCD testing procedure, which is a very important aspect of the large CCD testing operation planned for DES.

## 2.3. Electronics

For the CCD testing and characterization we have decided to use electronics as similar as possible to that used in the DES instrument. We consider that this is a relevant part of the testing project that will allow us to gain confidence in the operation of the devices with the instrument electronics, and will enable us to develop the tools and understanding needed to optimize the real system. The electronics of choice is the Monsoon system [7], a very flexible system specifically designed for controlling large mosaic arrays. The Monsoon system is now being considered as a candidate for the survey instrument, and the design of the full Monsoon based system is under development. The existing version, currently being used at Fermilab consists of a Master Control Board, a Clock and Bias Board and a CCD Acquisition Board (with 8 channels). The system is managed under an open source agreement and the user is provided with the documentation and specifications needed to build custom made boards that will fit in the Monsoon standard

and could be used to replace parts of Monsoon hardware. In this spirit the DES front end electronics group in designing a 12 channel acquisition board for Monsoon, that will be tested with DES CCDs in our facility at Fermilab.

We had a production version of the Monsoon system since 11/2005 and we were able to achieve the DES noise specification (readout noise  $< 10e$ ) shortly after that. However, this was done with a readout speed of  $\sim 90$  kpix/sec, more than a factor of 2 slower than that required for DES. We very quickly learned that the problem was due to the load that the CCD output was required to drive from the testing dewar to the controller (typically a coax cable of approximately 2 m). The problem was resolved by using an amplifier board mounted at the output of the dewar, and we can currently operate with noise significantly lower than  $10e$  and reading out at  $\sim 160$  kpix/sec. Currently efforts continue to reduce the readout time. The detailed noise studies are not presented in this document.

As one of the alternatives being considered for the Monsoon electronics, and also to have an independent check of our results, we also have in our CCD testing facility an Astronomical Research Cameras controller [8]. We have been able to obtain from this system a similar performance as that seen in the Monsoon controller. Our plan includes keeping this controller available for tests and crosschecks of the results obtained with Monsoon.

#### **2.4. Data collection and Database**

The images for CCD characterization are automatically collected using tcl/tk based software that communicates with the Monsoon Pixel Acquisition Node (PAN) via network sockets. This technology, part of the Monsoon software distribution, allows the user to implement any sequence of exposures in a very convenient manner. In addition to each image, a metadata file is produced with the information (exposure time, voltage setting, temperature, etc) for each image. The metadata information gets later stored in a image database that will provide access to the complete history of testing images for each device.

### **3. FULL CHARACTERIZATION**

The full characterization of the CCDs is done with the goal of finding the optimal operating parameters for these devices and determining if they satisfy the DES requirements presented in Table 1. The complete test done for a device include more than 400 images taken at different voltages (clock rails and bias) and for several illumination conditions. The complete set of images is taken automatically during a period of approximately 14 hours. The next sections of this document describes the steps that are included in our full characterization of a device.

#### **3.1 Photon transfer curve**

The photon transfer curve is obtained for each CCD by setting the operating voltages to our default and taking pairs of flat fields for each exposure time  $T_{exp} = 10, 20, 30, \dots, 400$ . The pairs of exposures at a given  $T_{exp}$  are then subtracted to obtain the variance and averaged for the calculation of the mean. This is the standard procedure to obtain gain for a device assuming a fixed electronic noise and poisson statistics for the number of photons as described in [9]. Fig. 3 shows an example of the results obtained with this method.

The data obtained in the photon transfer curve is also used to check the linearity in the response of the device. The DES specification for maximum nonlinearity is 0.1%. An example of results for the linearity studies are presented in Fig. 4.

An alternative method for obtaining the gain of the conversion factor between electrons and ADU (analog to digital units) is the Fe55 X-ray spectrum. In this case a X-Ray source (approximately  $100 \mu\text{C}$ ) in

presented to the CCD inside the dewar. This is possible because the dewar we are using has an knob accessible from the front face that when turned, presents the X-ray source to the front of the CCD (see Fig. 1). The resulting charge distribution for a 40 sec exposure to the source is presented in Fig. 5. The plot shows two main peaks, the leftmost one corresponding to the pedestal (only the dark electrons collected in the pixel) and the rightmost one corresponding to the signal from 1620 e produced by the X-ray emissions. The X-ray source has also a smaller fraction of higher energy emissions that produce yet another (much smaller) peak to the right of the 1620 e peak. For details on the spectrum expected from the Fe55 source see Ref. [9].

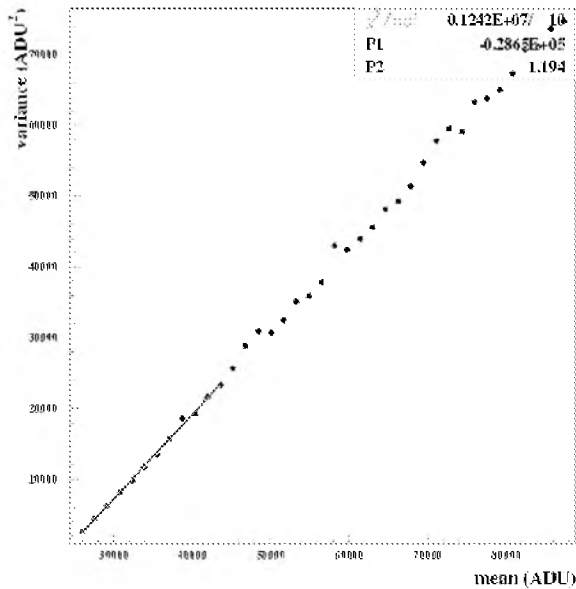


Fig. 3. Photon transfer curve. Variance as a function of mean obtained by taking a series of paired images with varying exposure time. The slope in this curve corresponds to the conversion factor in units of ADU/e. The fit indicates a gain of 1.19 ADU/e.

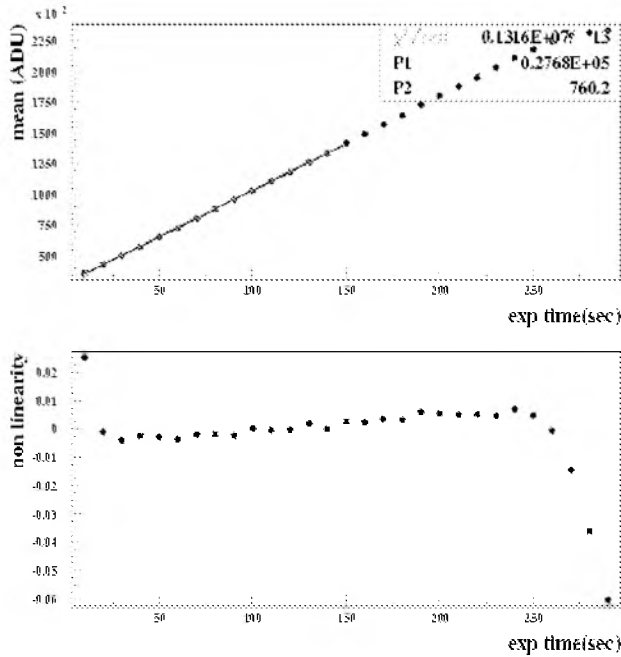


Fig.4. Linearity test. The mean a function of the exposure time is presented in the top panel. A linear fit is performed to exposure time less than 150 sec. Bottom: non linearity defined as the fractional difference between the points in the top panel and the fit. For this device the non linearity is less and 0.1% up to exposure times of 250 sec, which correspond to 225K ADU (16 bits provided by the Monsoon CCD board), the upper limit of the dynamic range of the electronics.

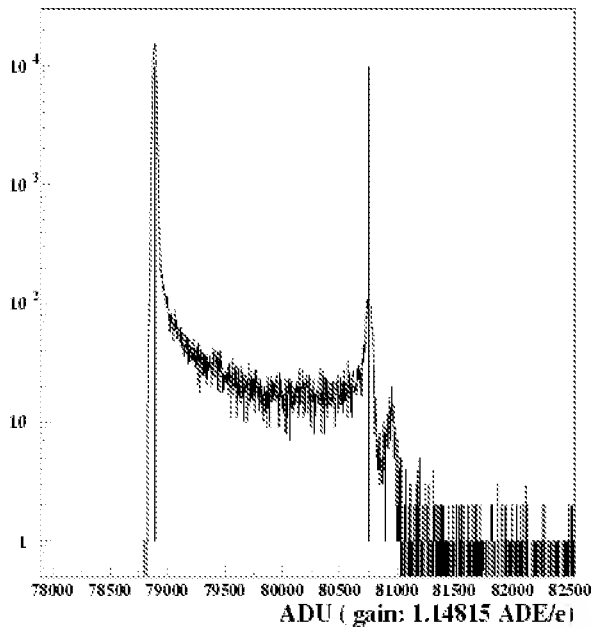


Fig.5. Charge distribution obtained for a 40 sec exposure to an X-ray source (Fe55,  $\sim 100 \mu\text{Curie}$ , 2 cm away from the surface of the device). The vertical lines indicate the pedestal position (left) and the peak corresponding to the 1620 e emission (right). The additional peak seen to the right corresponds to the higher energy emission from the source, and is not used to obtain the conversion factor

### 3.2 Clock rail optimization (Charge transfer efficiency)

As shown in Table 1, DES requirements include charge transfer inefficiency (CTI) less than  $10^{-5}$ . Part of our CCD characterization consists of studying the voltage needed for the clock rails in order to get this high transfer efficiency. For this measurement, we take flat exposures with fixed illumination (about 10000 e per pixel), and changing the voltage levels for the horizontal phases. The transition between the exposed pixels and the horizontal overscan region is then studied for these images, as shown in Fig. 6. The sharpness in the edge of this transition is an indicator of the charge transfer efficiency. The result for the CTI as a function of the positive side of the horizontal clock (H+) phases is shown in Fig. 7. For the device shown in the figure, the CTI specification for DES is satisfied when H+ is higher than 6.5 V.

The negative side of the horizontal clocks (H-) is studied in an analog way, by fixing the H+ to a high value and changing H-. The results obtained typically indicate the CCD will have good CTI for H- < 2.0 V

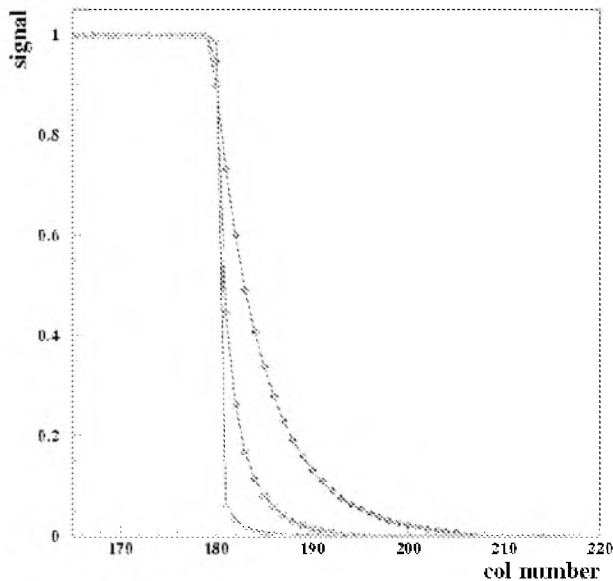


Fig. 6 Transition between the overscan and the exposed pixels. The horizontal overscan starts at column number 181 in this plot. For a perfect transfer efficiency the transition between the exposed area (col < 181) and the overscan (col  $\geq$  181) should be perfectly sharp, going from 1 to 0 in this scale. Note that the y-axis has been normalized to obtain 1 in the exposed region and 0 in the overscan, away from the transition area (col < 210). The different colors represent the transition for different levels for the H+ clock, and one can see that this transition can be either very slow or extremely sharp depending on this voltage. The curves show the edge for voltages H+ = 4.5V, 5V and 5.5 V (the sharpest transition corresponding to the higher voltage).

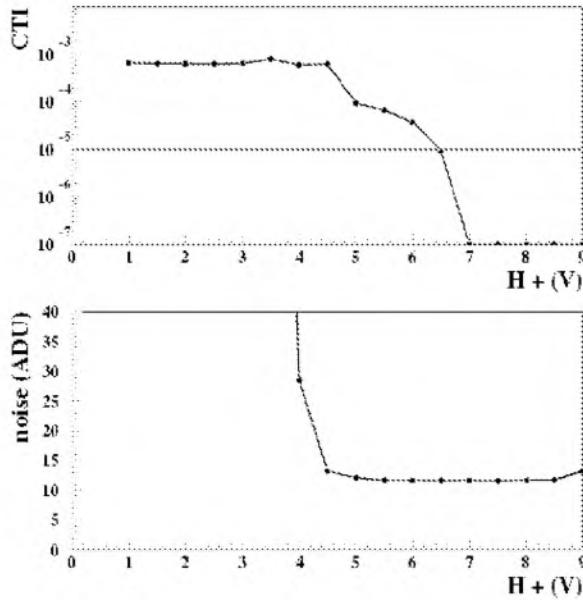


Fig. 7. Top) Charge transfer inefficiency as a function of the positive rail for the horizontal clock phases. The horizontal line indicates the DES specification, and one can see that this device satisfies the requirements for  $H^+ > 6.5$  V. Bottom) The plot shows the RMS noise as a function of  $H^+$ , the noise is measured in the overscan region and for this reason when there is a large CTI the measurement is not well defined. However, the plot clearly shows that once we have a low CTI the noise is stable in this range of  $H^+$  voltages.

The vertical clock voltages are also investigated in order to understand at which voltage the device will perform according to the DES specs, see Table I. In a way similar to that presented above, the edge of the CCD is studied, in this case the transition between the vertical overscan and the exposed area. In general for these devices we obtain vertical  $CTI < 10^{-5}$  for vertical rails  $V^+ > 6V$  and  $V^- < -3V$ .

### 3.3 Output gate transfer curve ( $V_{Thr}$ )

Also part of our full characterization for each CCD is the measurement of the output transfer gate curve, as described Ref.[4]. The goal is to measure the voltage at which charge injection is produced in the device as a function of  $V_{ref}$ . This technique allows the determination of the channel voltage inside the CCD, under the output gate. Charge injection occurs when this voltage is lower than the  $V_{ref}$ , the difference between the applied gate voltage and the channel voltage is typically called  $V_{th}$  and depends on the doping conditions of the silicon. We use this measurement to understand the uniformity of our devices. An example of the results obtained for one device is shown in Fig. 8.

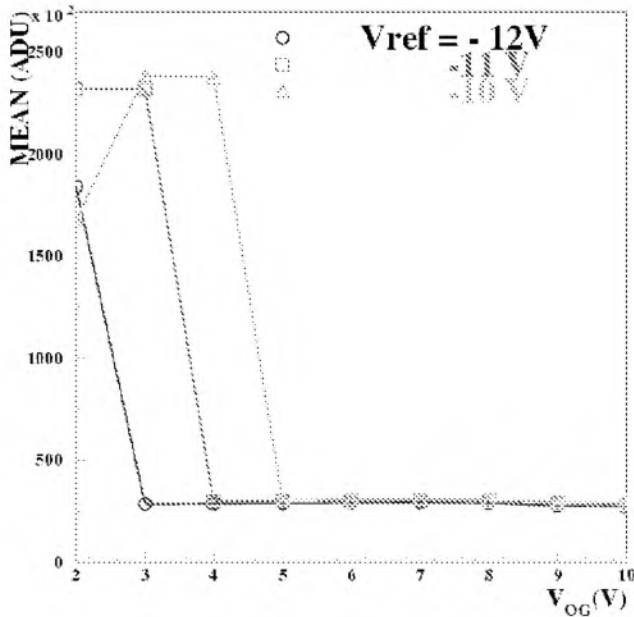


Fig. 8. The curves show mean ADU measured as a function of the output gate voltage ( $V_{OG}$ ) for different values of the reference voltage. When charge injection is produced the electronics saturates and we see large deviations from the pedestal value ( $\sim 25000$  ADU). In this example charge injection occurs for  $V_{OG} < 3V$  when  $V_{ref} = -12V$ , which indicates  $V_{th} = 15V$ .

### 3.4 Cosmetics

Before dicing, the DES CCDs are tested at  $-45C$  at the LBNL facility. The results from the testing at  $-45C$  indicate if the device is functional (video signal coming out and charge moving inside the device) without measuring detailed performance, and also provide a count of defects. A detailed list of defects is done from the data collected in this cold probing station. This preliminary list of defects is used for establishing a packaging priority and separating the devices that have science potential from the rest. Before packaging, the devices are further inspected by eye under a microscope and the visible defects are documented. Our full characterization gives yet another list, this time definitive, about defects and cosmetics problems in our packaged devices. The combination of the defects observed at different steps in the production becomes an important tool to detect possible evolution of the imperfections in the devices.

### 3.5 Dark Counts

The dark counts were studied in a DES CCD which satisfied all the rest of our DES requirements. The number of electrons detected per pixel is shown in Fig. 9 as a function of temperature. The original DES spec of  $25$  e/pix/hour is shown as the horizontal line here. In order to achieve this specification we need to cool down below  $150$  K. The dark current specification is currently under because we could gain  $\sim 15\%$  in QE around  $1000nm$  if we could operate at  $165K$  instead, which could have a significant impact in our efficiency for the observation of high redshift targets in the survey.

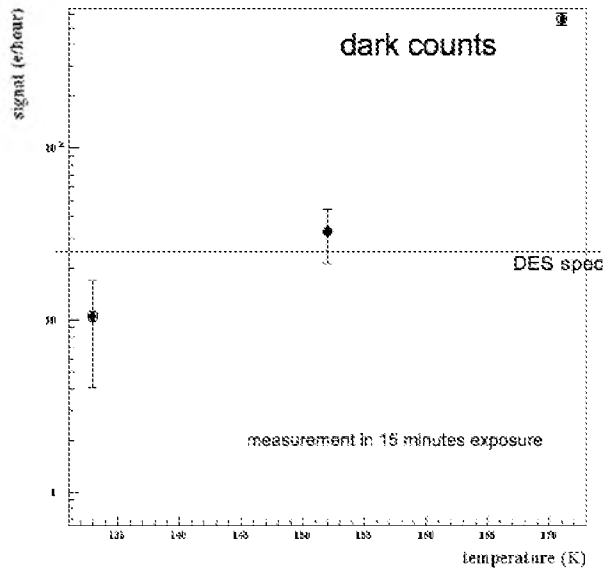


Fig. 9. Dark counts in  $e/(\text{pix hour})$  as a function of operating temperature for device that satisfies all the other DES requirements presented in Table 1. The horizontal line shows the DES spec of  $25 e/(\text{pix hour})$ .

### 3.6 Quantum efficiency

As mentioned above a key feature of our detectors for the success of the DES project is the high efficiency in the near infrared [3,6]. This efficiency is verified in our testing facility using a calibrated photodiode and a monochromator. The calibrated photodiode is mounted at one of the output ports of the integrating sphere, with the other port connected to the CCD. This method gives the relative Q.E. of the CCD as a function of wavelength, in order to obtain the absolute QE, a device with known response will be installed inside the dewar. The results for relative QE as a function of wavelength is shown in Fig. 10.

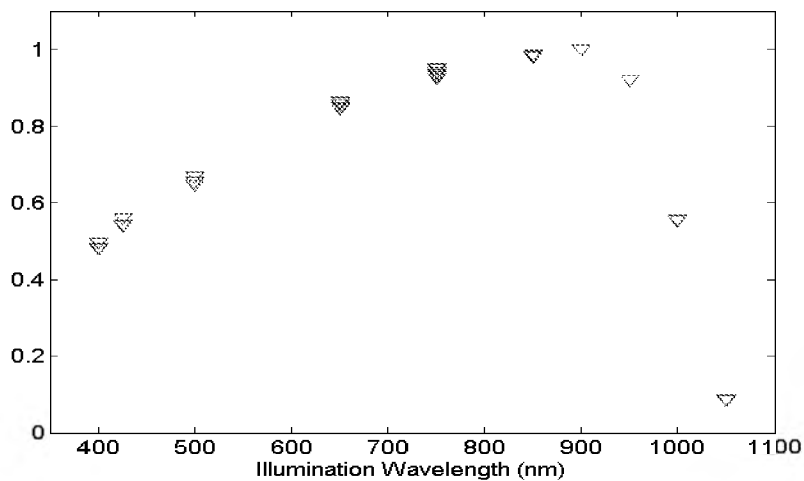


Fig. 10. Results of relative QE as a function of wavelength for a DES device. The measurement presented here is normalized to the peak efficiency seen at  $\sim 900$  nm. These results demonstrate that the CCD shows the highest efficiency around 900 nm, as expected for the fully depleted  $250 \mu\text{m}$  detector.

### 3.7 Diffusion

The diffusion specification for the CCDs in the DES focal plan is  $\sigma_{\text{diff}} < 7 \mu\text{m}$ , this requirement comes from the maximum PSF in the instrument that can be allowed without compromising the science output of the survey. The diffusion for CCDs built with the same technology than those we plan to use for DES has been characterized in great detail in previous work [10]. The previous measurements were performed using the “spot-o-matic”, an optical apparatus that focuses a small light spot ( $\sim 30 \mu\text{m}$ ) with known profile over the surface of the CCD, and that allows a very fine control of the position of that spot. The diffusion is then calculated by measuring that charge collected in the pixels inside a region of the CCD as a function of the light spot.

At DES we have developed an alternative method for doing this measurement that does not involve focusing a very small spot of light onto the CCD. This method has an advantage for us, because it can be implemented as part of our routine testing without having to install the devices in a testing station dedicated exclusively to diffusion measurements.

The idea is to project a diffraction pattern into the surface of a CCD and measure the diffusion as a change in the contrast of this pattern. The diffraction is produced by a double slit (built at Fermilab and mounted on our system using the ORIEL standard flanges). The slit is illuminated with a pulsed laser (HeNe). A typical image of the diffraction pattern obtained is shown in Fig. 11.

The Fourier transformation of the region of the CCD with this image is obtained as shown in Fig. 12. As the effect of diffusion becomes more significant the amplitude in the peak in the fourier power spectrum is reduced. Introducing diffusion has the effect of multiplying the power spectrum of the original image by a Gaussian in the wave number  $k$ , centered at 0 with width equal to  $1/\sigma_{\text{diff}}$ . As discussed in [10], for high substrate voltages the diffusion follows the relation  $\sigma_{\text{diff}}^2 \propto V_{\text{sub}}$ . Using this expression, and the measured decrease in the peak of the Fourier spectrum as a function of voltage one can determine the diffusion of the device under test as a function of  $V_{\text{sub}}$ , the results are shown (and compared with results from previous work [10]) in Fig. 13.

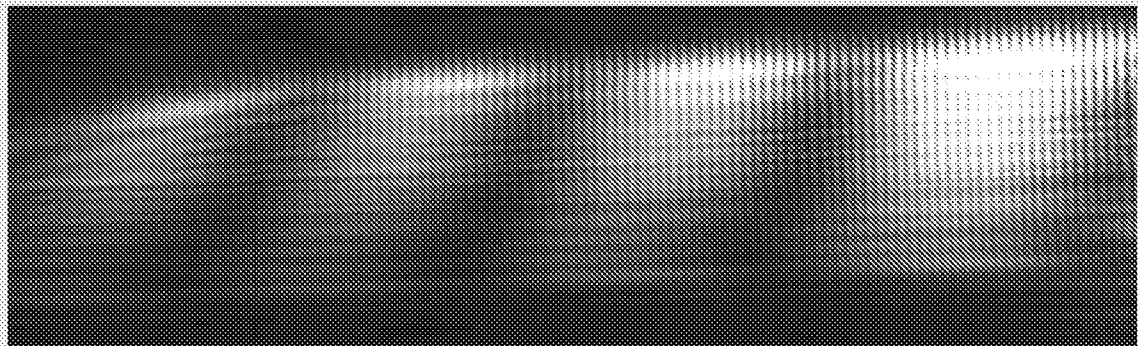


Fig. 11. CCD image of the diffraction pattern produced for diffusion studies. The pattern is produced with a double slit and illuminated with a pulsed He-Ne laser.

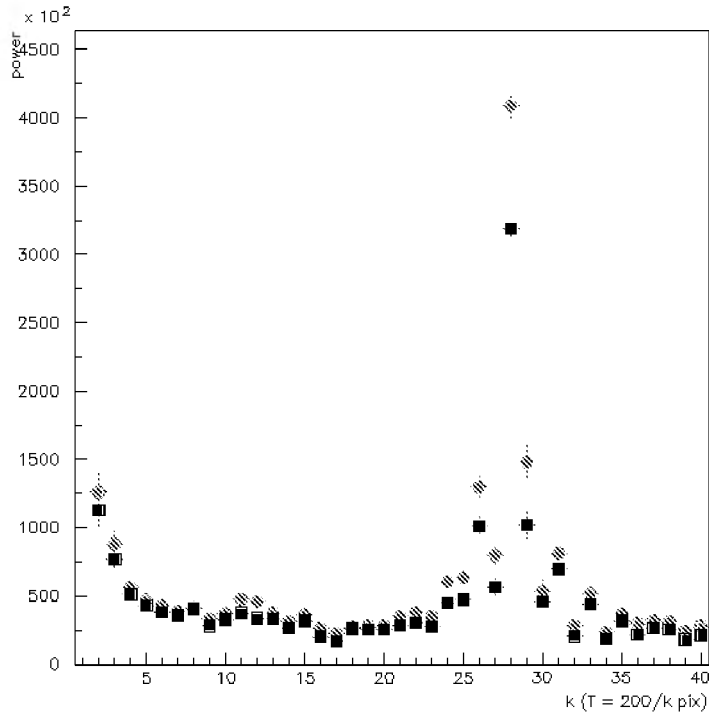


Fig. 12. Power as a function of wavenumber for the diffraction pattern presented in Fig 11. The circles correspond to  $V_{sub}=30$  V and the squares correspond to  $V_{sub}=40$  V. The peak in the wave number corresponds to an oscillation with period 7 pixels.

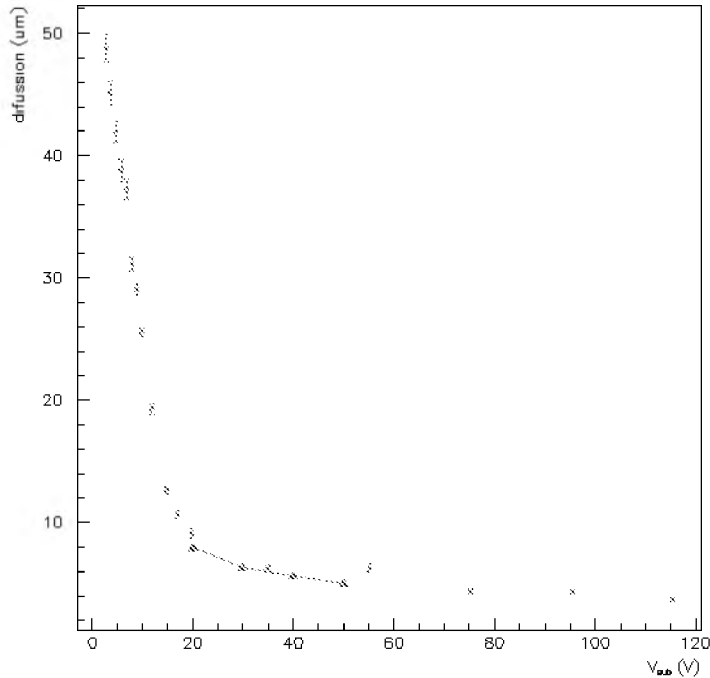


Fig. 13. Diffusion calculation from the diffraction pattern method, the triangles joined by line compared with the detailed measured of the diffusion performed in previous work [10].

### 3.8 Flatness measurements

For those devices that satisfy the requirements in Table 1, which we consider to be of science grade, an additional testing step will be performed. This test will evaluate the flatness of the CCD in its pedestal package. Significant deviations of the focal plane from a perfect flat surface will cause degradation in the image, and will affect the PSF of the instrument. The flatness measurement is done in our CCD testing facility using the commercial flatness measurement instrument [11] that is composed of an illumination source with an intentional large chromatic aberration (different wavelengths are focused at different distances from the source) and an spectrometer that is used to identify which frequency is being focused at a given surface. Details of the method and results obtained are presented in Ref. [5].

#### **4. RESULTS AND CONCLUSION**

The CCD testing facility at Fermilab has been built and significant device studies for DES have been done. We now have the tools for testing the detectors for the DES focal plane and to certify them as passing the minimal requirements established for the operation in the survey instrument. This has been achieved using the readout electronics that we plan to use for the DES instrument (Monsoon readout system).

We have fully characterized 15 CCDs of the type that will be used for imaging in the DES instrument, and operated a total of 30 2k x 4k devices (and a somewhat smaller number of devices with other dimensions). All the devices tested have been selected not to have scientific potential due to cosmetic defects or other problems. The pedestal package for the DES CCDs is being developed and will be available during 2006. At this point we will begin testing of the devices whose cold probe data suggest they have the potential to be part of the focal plane (we do not want to package those devices a way that will not be compatible with the final design of the DES focal plane).

From the tested devices we have been able to conclude that it is possible to group CCDs in the focal plane in sets of 3 and share the clock levels among them, without comprising the performance of the survey instrument. There is actually a unique set of voltages that will work for all the devices that satisfied the DES requirements, which will indicate that the groups sharing the clock levels could be larger than 3, simplifying the electronics design. However, given the small number of devices tested and considering that they come only from the first two lots, we consider inappropriate to design our instrument with less flexibility in the setting of voltages. This aspect will continue to be under study by the DES collaboration.

We have learned that in order to operate the CCDs at the noise and readout time needed by DES we will need to install an amplifier close to the device. This is an important aspect of the instrument design that we needed to define as early as possible.

We have been able to verify that the LBNL devices will satisfy all the requirements for DES, but since we have selected not to operate yet those devices with scientific potential we do not have a good estimator for the yield, but our results are consistent with the 25% estimation from other production runs.

#### **Acknowledgments**

This work was supported in part by the University of Illinois and the U. S. Department of Energy under contract No. DE-FG02-91ER40677.

#### **References**

1. The DES Collaboration, The Dark Energy Survey whitepaper; submitted to the Dark Energy Task Force June 2005, astro-ph/0510346. Additional whitepapers on Theoretical & Computational Challenges, submitted to the Dark Energy Task Force Sept. 2005, astro-ph/0510194,5; also available on the web: [https://www.darkenergysurvey.org/the-project/survey\\_documents/DES-DETF/](https://www.darkenergysurvey.org/the-project/survey_documents/DES-DETF/).

2. T. Abbott et al, "The CTIO V. M. Blanco 4-m Telescope and the Dark Energy Survey", these proceedings.
3. "The Dark Energy Survey Instrument Design", Brenna Flaugher for the DES Collaboration, These proceedings.
4. S.E. Holland, D.E. Groom, N.P. Palaio, R. J. Stover, and M. Wei, "Fully Depleted, Back-Illuminated Charge-Coupled Devices Fabricated on High-Resistivity Silicon," IEEE Trans. Electron Dev. **50** (3), 225--238 (January 2003) LBNL-49992
5. G. Derylo for the DES Collaboration, "The Status of 0.250mm-Thick CCD Packaging for the Dark Energy Survey Camera Array", these proceedings
6. The DES Collaboration, "A Proposal to NOAO for the Dark Energy Survey", [https://decam.fnal.gov/NOAO04/A\\_Proposal\\_to\\_NOAO.pdf](https://decam.fnal.gov/NOAO04/A_Proposal_to_NOAO.pdf).
7. More information about the Monsoon readout system: <http://www.noao.edu/ets/monsoon/>
8. More information about the Astronomical Research Cameras readout system can be found at <http://mintaka.sdsu.edu/arc/index.html>
9. J.R. Janesick, Scientific Charge-Coupled Devices, Springer 2001.
10. A. Karcher, C.J. Bebek, W. F. Kolbe, D. Maurath, V. Prasad, M. Uslenghi, M. Wagner, "Measurement of Lateral Charge Diffusion in Thick, Fully Depleted, Back-illuminated CCDs," IEEE Trans. Nucl. Sci. **51** (5) (2004) LBNL-55685; Jessamyn A. Fairfield "Improved spatial resolution in thick, fully depleted CCDs with enhanced red sensitivity," in Proc. IEEE Nucl. Symp. Med. Imaging Conf., Nov. 2005.